

# Optical resistance of sapphire

A. CHMEL, S. B. ERONKO, A. M. KONDYREV, V. YA. NAZAROVA

*A. F. Ioffe Physico-Technical Institute, Academy of Sciences of Russia, 194021 St Petersburg, Russia*

Single-crystals of  $\alpha$ -Al<sub>2</sub>O<sub>3</sub> were subjected to multi-stage polishing with diamond powder of successively decreasing grain size. After each stage of polishing, the infrared reflection spectra were recorded and the nanosecond laser resistance at 1.06  $\mu$ m was measured. The laser-induced damage data were also obtained for natural face, annealed and ion-etched surfaces. It was shown that (i) disorder of the crystal structure affects the optical resistance, resulting in a decrease of damage threshold, and (ii) the surface layer disturbed by grinding retains a "memory" of the initial structure. The multi-pulse sub-threshold laser irradiation which leads, finally, to macroscopic damage of a sample, stimulates the process of structural ordering, together with the formation of "dangerous" local defects.

## 1. Introduction

Sapphire is a widely used optical material, but its laser-induced damage (LID) has been little studied. Some problems, for example, temperature dependence of optical resistance and multiple-pulse LID phenomena, thoroughly investigated in glasses, crystalline SiO<sub>2</sub>, and alkali-haloid crystals, have not been studied in sapphire. There is also a number of problems connected with the processing of the  $\alpha$ -Al<sub>2</sub>O<sub>3</sub> crystals provided for the laser apparatus.

This paper reports the experimental results of LID and optical resistance investigations performed on sapphire. It was found that the accumulation of irreversible changes in  $\alpha$ -Al<sub>2</sub>O<sub>3</sub> under the sub-threshold irradiation is an ambiguous process; it coexists with simultaneous ordering of the crystal structure of a sample. Much attention is paid to the surface damage of sapphire because the laser apparatus serviceability and reliability are conditioned in many cases by the surface optical strength of power-optics units. In connection with the practical value of the latter problem, some recommendations are made for optimization of the polishing procedure of sapphire samples.

Investigation of structural transformation in the material subjected to mechanical treatment and laser radiation was performed using infrared reflection spectroscopy, which is rather sensitive to defects in the  $\alpha$ -Al<sub>2</sub>O<sub>3</sub> crystal lattice [1].

## 2. Experimental procedure

### 2.1. Samples

$\alpha$ -Al<sub>2</sub>O<sub>3</sub> monocrystals were grown in the Vavilov State Optical Institute by the Kyrospulos modified method (KMM) developed by Musatov [2] for large-size crystal preparation. The specificity of this method is that the growth and annealing of the crystal is performed just inside the tungsten–molybdenum crucible without subjecting the crystal to the temperature-gradient zone above the crucible. The melt is

then cooled as the temperature of the crucible decreases. Owing to low residual stresses and the low density of dislocations, the single crystals prepared by the KMM have high optical quality. In addition, when the  $\alpha$ -Al<sub>2</sub>O<sub>3</sub> crystal is grown by the KMM, its natural face is formed perpendicular to the principal axis, which allows estimation of structural ordering by infrared spectroscopy: the interpretation of the spectra supported by the theoretical group analysis is known only for faces (0001) and (1010) [1]. The unpolished natural face may be taken as a standard to evaluate the performance of polishing.

Samples prepared by the Verneuil technique were also used. Verneuil crystals have no oriented face of growth suitable for spectroscopic studies. Moreover, due to some peculiarities of the method, residual stresses, dislocation density, block structures were more developed in Verneuil-grown crystals than in KMM-prepared ones. At the same time, Verneuil-grown samples contain fewer metallic impurities, because no tungsten heater or crucible were used.

The polishing conditions will be described later. In those cases when the method of crystal growth is not stated, the KMM was used.

### 2.2. Equipment

#### 2.2.1. Light sources

To obtain a more complete picture of the laser light interaction with sapphire, three sets of equipment having different parameters were used.

(i) A YAG:Nd<sup>3+</sup>-laser operating with a single axial mode TEM<sub>00</sub>. The single-mode condition was provided by using a circular travelling-wave resonator with the field rotated. Single-frequency operation was achieved by placing the Fabry–Perot echelon into the resonator. The output power,  $U_0$ , was 0.07 J. Reproduction of pulses in intensity was better than 95%, and the pulse repetition frequency,  $f$ , was 1 Hz with a pulse duration  $t_p = 30$  ns. The beam was focused to a

spot of 13  $\mu\text{m}$  effective diameter,  $d_{\text{eff}}$  ( $d_{\text{eff}}$  corresponds to the diameter at which the power is  $1/e$  times its maximum value). This apparatus is called "laser 1".

(ii) Single-mode, single-frequency neodymium glass laser, comprising a master generator and three amplifying stages.  $U_0 \sim 1 \text{ J}$ ,  $d_{\text{eff}} = 10 \text{ mm}$ ,  $t_p = 20 \text{ ns}$ , periodicity 1 pulse in 5 min (laser 2).

(iii) Q-switched YAG:Nd<sup>3+</sup> laser with transverse-mode selecting.  $U_0 = 0.3 \text{ J}$ ,  $f = 1 \text{ Hz}$ ,  $t_p = 60 \text{ ns}$  (laser 3). This laser has a worse energy distribution in the pulse than 1 has laser, but it provides power radiation in a greater focal spot.

The energy of the pulses was reduced to the required value by neutral light filters.

### 2.2.2. Infrared reflection spectra

Spectroscopic measurements were performed on the grating IR spectrophotometer Jasco Model DS403G equipped with an attachment for obtaining an external reflection spectrum from a surface area of 3 mm<sup>2</sup>. Because of the small focal spot provided by laser 3, radiation was directed on to the surface as required for registering the infrared spectrum by step scanning. To estimate the gradient of structural distortion in the grinding-modified layer, in addition to the external reflection spectra, the attenuated total reflection (ATR) spectra were also measured. When the external reflection spectrum is recorded, the incident beam falls on a sample from the air, while in the case of the ATR technique, the infrared light falls from the prism having a higher refractive index than that of the sample. The greater the refractive index of the prism, the lower is the light penetration depth. In our ATR measurements, we used a prism made of single-crystalline tellurium which is transparent in the middle-infrared range and has a refractive index of 6.3 along the main optical axis. The ATR spectrum of  $\alpha\text{-Al}_2\text{O}_3$  obtained with the help of this prism, corresponds to a layer  $\sim 0.2 \mu\text{m}$  thick. The infrared external reflection spectrum provides information on a layer 0.4–0.7  $\mu\text{m}$  thick, depending on the depth of light penetration into the sapphire at various frequencies.

The true frequencies of the atomic vibrations in a crystal correspond to the peaks of the function of the imaginary part of dielectric permittivity,  $\varepsilon''(\nu)$ . The frequency dependences (the spectra) of  $\varepsilon''$  were determined by Kramers–Kronig analysis.

In order to use the Kramers–Kronig calculation procedure, the reflection spectra must be recorded over a wide frequency range. In our experiment, the spectra were measured in the range 1300–200  $\text{cm}^{-1}$ , but for convenience, only their fragments in the vicinity of the structurally sensitive band at 570  $\text{cm}^{-1}$  will be shown in the figures in most cases. The band frequencies are denoted in all cases according to their position in the  $\varepsilon''(\nu)$  spectrum.

## 3. Results and discussion

### 3.1. The modified layer on a polished crystal

#### 3.1.1. Grinding and polishing

Grinding of a hard material such as sapphire, is accompanied by high pressure and temperature be-

tween the treated surface and the powder grain. The action of pressure and heating on a crystal may be revealed as plastic deformation, increase in concentration of thermodynamic defects, and development of polycrystalline structure.

Defects in crystalline structure manifest themselves in the infrared spectrum. Fig. 1 represents the experimental reflection spectra and the calculated functions  $\varepsilon''(\nu)$ , obtained for the natural face and for the respective coplanar polished surface of the same sample. In the spectra of the latter, the intensity of the band at 570  $\text{cm}^{-1}$  is much smaller, but the half-width is greater than that in the spectrum of the natural face. In addition, a low-frequency shift of the band maximum is observed. The calculated  $\varepsilon''(\nu)$  spectrum of the polished surface belonging to the layer 0.2–0.3  $\mu\text{m}$  thick, differs from that of the natural face to a greater degree than the spectrum of the polished surface measured at an infrared light penetration depth of 0.4–0.7  $\mu\text{m}$ .

After annealing at 1900 °C for 1 h in a vacuum of  $10^{-5}$  torr (1 torr = 133.322 Pa), the spectrum of the polished surface was found to be nearly the same as the spectrum of the natural face. Ar<sup>+</sup>-ionic etching, which removes a surface layer of 0.8  $\mu\text{m}$  thick, results in further increase of intensity of the 571  $\text{cm}^{-1}$  band.

Changes observed in the infrared spectra are typical for the transition of a crystalline phase to the amorphous state. Sapphire has no thermodynamically equilibrium stable amorphous phase. Therefore, grinding leads to the appearance of non-equilibrium disordered layer, which only conditionally may be called an "amorphous film" [3].

The spectrum of the polished plane reveals an additional weak band at  $\sim 590 \text{ cm}^{-1}$ , which indicates the existence of local deformations in the crystal lattice [1], caused by the mechanical treatment of the surface. High-temperature annealing leads to partial evaporation and relaxation of the layer, and the treated surface again becomes as perfect as the natural face.

#### 3.1.2. Optical resistance

A defective layer existing on the polished surface, obviously influences the laser resistance of a crystal [4, 5]. Table I gives the optical strength values measured for both the surface (for the corresponding spectra see Fig. 1) and for the bulk of a sample. Optical strength was determined as the threshold power density in a pulse,  $Q_{\text{th}}$ , for which the probability of a plasma flare arising after a single shoot is 0.5 (Fig. 2). The single-pulse damage threshold of any surface is much smaller than the bulk damage threshold. At the same time, the optical strength of the natural face is markedly higher than that of the polished plane, but it is slightly smaller than the optical strength of the polished surface of the annealed sample. The ion-etched surface reveals a higher resistance to laser radiation. Because the natural face and the annealed or ion-etched polished surface are spectroscopically (i.e. in this case, crystallographically) identical, the difference in their optical strength may be explained by (i) the difference in the surface profiles [6] (the natural face has micro-

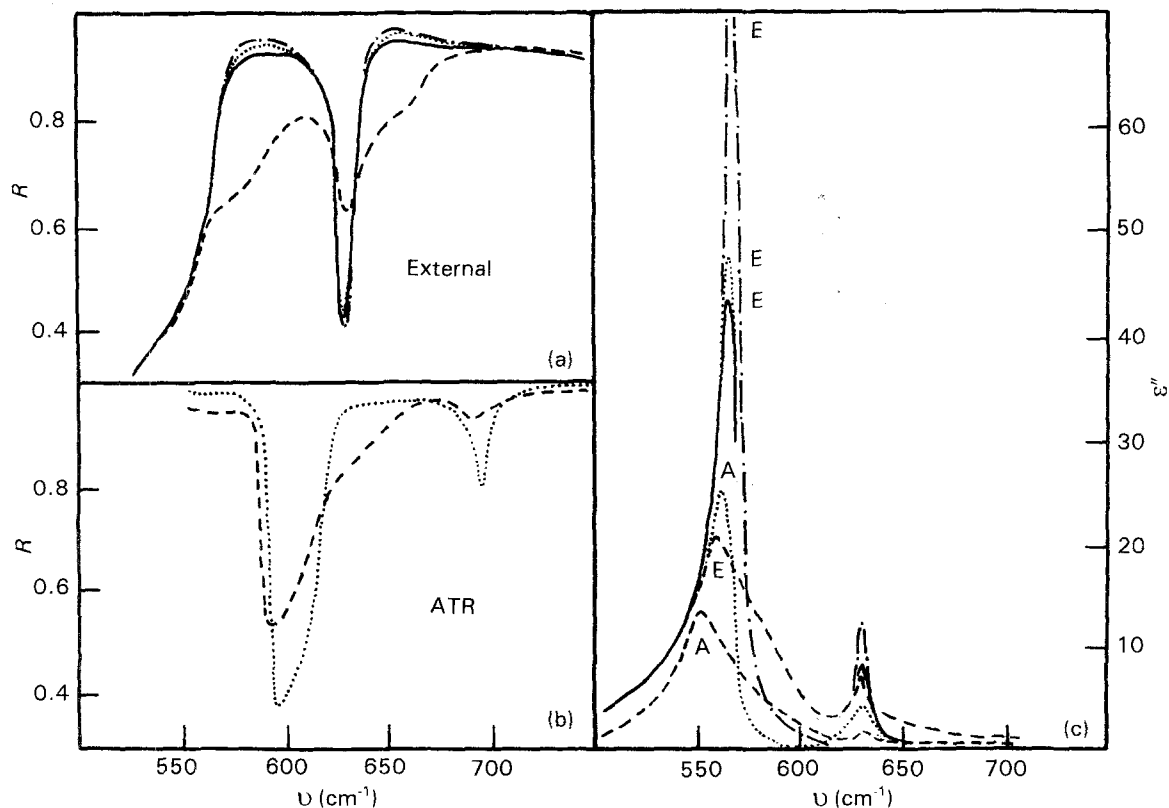


Figure 1 (a) Infrared external reflection, (b) ATR spectra, and (c) their functions  $\epsilon''(\nu)$  which are designated "E" and "A", respectively. (—) Natural face, (---) polished, (···) annealed, (— — —) ion-etched.

TABLE I Single-pulse damage threshold power density in the bulk and on the surface of  $\alpha$ - $\text{Al}_2\text{O}_3$

Laser-beam focusing	$Q_{th}$ (rel. units)
Bulk	1.0
Polished surface	0.15
Polished, annealed at 1900 °C surface	0.5
Polished, ion-etched surface	0.8
Natural face of a crystal	0.4

steps of heights up to  $10^2 \mu\text{m}$ , while the profile of the polished plane does not exceed  $1 \mu\text{m}$ , and (ii) accumulation of impurities on the growing face during crystal preparation. Annealing relieves the local stresses and partially removes the layer distorted by grinding, thus exposing the bulk of a sample.

The thickness of the modified layer can also be varied during "deep" polishing. It is well known that the polishing conditions influence the optical resistance of glasses [6, 7], but for  $\alpha$ - $\text{Al}_2\text{O}_3$  such data have not yet been reported. Because the dependence of the optical strength on the material processing conditions is of practical interest, we studied in detail the polishing process of sapphire from the viewpoint of achieving higher strength.

The sapphire plates were cut normal to the crystalline axis. The planes of the samples were polished with diamond powders, the powder grain size being successively decreased as follows: 40/28  $\rightarrow$  5/3  $\rightarrow$  3/2  $\rightarrow$  1/0  $\rightarrow$  0.5/0  $\rightarrow$  0.3/0  $\rightarrow$  0.1/0  $\mu\text{m}$ . For powders 40/28 and 5/3  $\mu\text{m}$ , the duration of treatment was 2 h, for the other powders it was 1 h for each particle

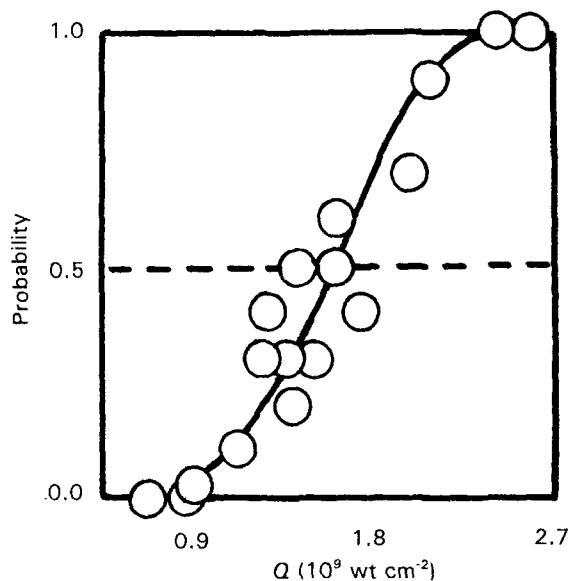


Figure 2 Probability of damage events on the surface of the natural face of a single crystal depending on the power density in a pulse.

size. Under these conditions, each subsequent stage of polishing completely removes the surface layer which was disturbed during the previous stage. Before changing the powder for the next one, the infrared reflection spectrum was recorded and the optical strength was measured.

Fig. 3 represents the spectra obtained for the sample subjected to multi-stage polishing, and also for the natural face. As the surface is multi-stage treated, the spectra vary in a complicated way. There are four peaks at 385, 441, 570 and 637  $\text{cm}^{-1}$  (the frequencies

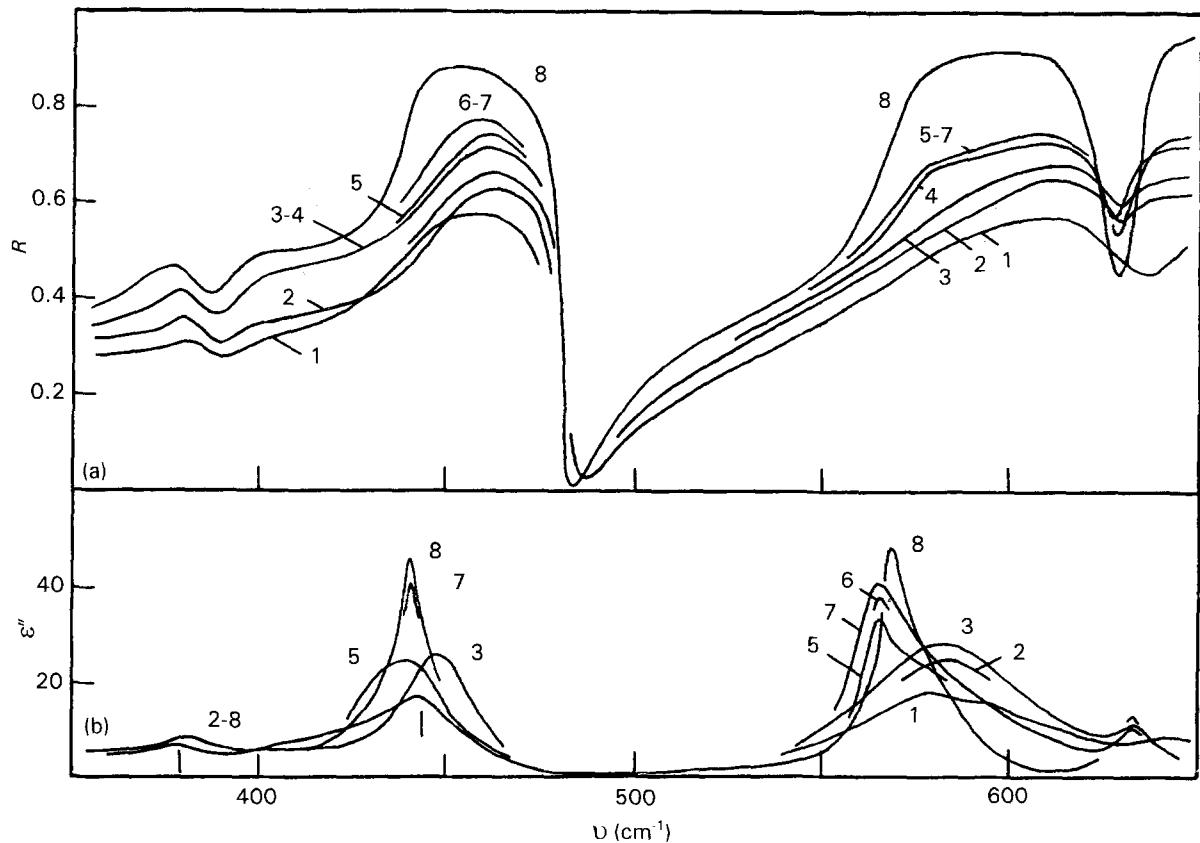


Figure 3 (a) Infrared reflection spectra and (b) calculated functions  $\epsilon''(\nu)$  of the (0001) face after grinding with diamond powders (1-7) and those of the natural face. Numbers 1-7 indicate the relevant stages of treatment: 1, 40  $\mu\text{m}$  grit; 2, 5/3  $\mu\text{m}$  grit; 3, 3/2  $\mu\text{m}$  grit; 4, 1/0  $\mu\text{m}$  grit; 5, 0.5/0  $\mu\text{m}$  grit; 6, 0.3/0  $\mu\text{m}$  grit; 7, 0.1/0  $\mu\text{m}$  grit; 8, natural face.

are given in the order in which the bands are positioned in the spectrum of the natural face) in the spectrum  $\epsilon''(\nu)$ . As the powder grains are used in decreasing size order, the intensity of the bands increases and the maxima shift. Fig. 4 shows histograms of peak positions,  $\nu_{\text{max}}$ , for the two most intense bands at 441 and 570  $\text{cm}^{-1}$  for each stage of treatment of the sample. The band frequencies display an increase at the second stage, then they decrease, achieving the lowest values when the powder of 0.5/0  $\mu\text{m}$  particle size is used. The variation of the infrared peak frequencies is connected with changes in the physical and geometrical parameters of the surface-modified layer under the mechanical treatment.

Geometrically, the modified layer may be characterized by its thickness,  $d_m$ , and by the surface roughness, i.e. by the relief height,  $R_z$ . A rough estimate for the former parameter is given by the approximate relation:  $d_m \approx 1.5 D_p$  [8], where  $D_p$  is the diameter of the abrasive particles. Another dependence, i.e.  $R_z$  versus  $D_p$  is not linear. If  $D_p$  is less than  $\sim 1 \mu\text{m}$ , the relation  $R_z \approx 10^{-2} D_p$  is valid. At greater  $D_p$ ,  $R_z$  varies from  $0.1 D_p$  to  $0.3 D_p$  depending on the grinding conditions [9, 10].

We have evaluated the parameters  $d_m$  and  $R_z$  for all stages of the treatment procedure and compared them with the penetration depth of the reflecting infrared probe beam,  $D_0$ , at frequencies of the most intense bands at 441 and 570  $\text{cm}^{-1}$ . The semi-quantitative nomogram obtained is shown in Fig. 5. There are two peculiar points in this schedule. One of them is the

intersection of the plot of  $d_m$  versus  $D_p$  with the lines  $D_0 = \text{const.}$  at  $D_p = 0.5 \mu\text{m}$ . The other point lies in the region  $D_p = 5-40 \mu\text{m}$ , where the lines  $D_0 = \text{const.}$  are intersected by the  $R_z$  versus  $D_p$  plot. The first intersection coincides with the minima of the band frequencies in the histograms (Fig. 4). The second one corresponds to the appearance of maxima in the dependence of  $\nu_{\text{max}}$  on  $D_p$ .

Thus, the peaks of the function  $\epsilon''(\nu)$  shift due to both strains induced by polishing, and to changes in the geometry of the spectroscopic experiment during processing. At the first stage (grinding with powder of 40/28  $\mu\text{m}$  grain size), the roughness of the surface is more than the infrared light penetration depth (Fig. 5a and b). The condition of specular reflection is not valid in this case, and the spectra recorded do not respect the true ones. Therefore, the first maximum in histograms of the band positions does not correspond to any particular change in the properties of a sample. In the interval  $0.5 \mu\text{m} < D_p < 5 \mu\text{m}$  (Fig. 5a and c), the decrease in the  $\epsilon''(\nu)$  peak frequencies adequately reflects the lattice deformations induced by grinding. As the particle size decreases, the strain grows. If the size is less than 0.5  $\mu\text{m}$ , the light penetration depth exceeds the modified layer in thickness (Fig. 5a and d). In this case ( $D_0 > d_m$ ), the bulk of a sample contributes to the reflection spectrum. The contribution of the undistorted region increases with subsequent decrease of  $d_m$ , resulting in the reverse shift of the infrared bands.

The distorted layer itself is very inhomogeneous. In Fig. 6a one can see the evolution of the 570  $\text{cm}^{-1}$  peak

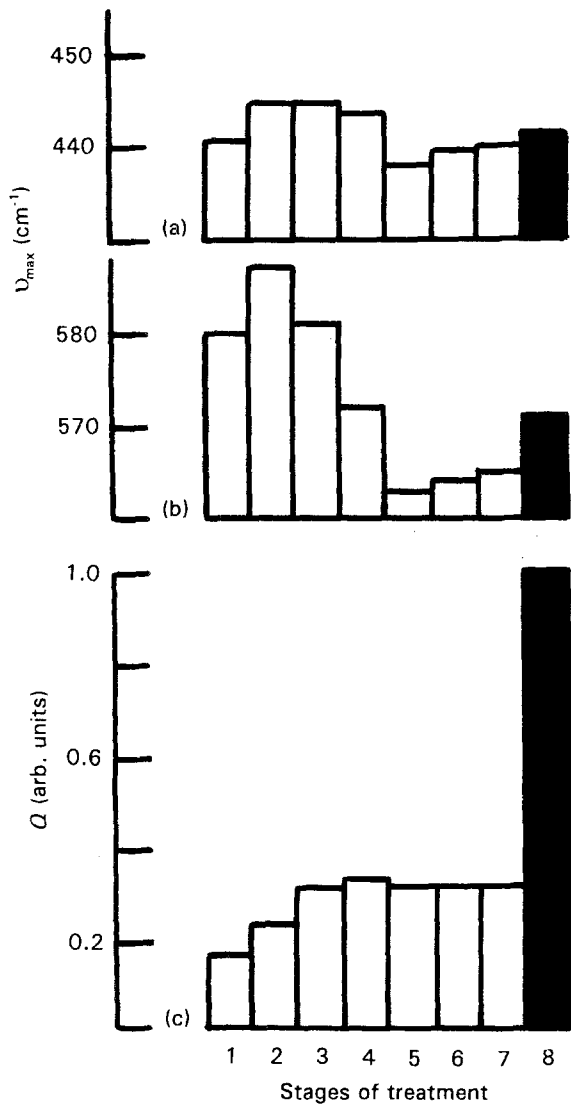


Figure 4 Histograms of the  $\nu_{\max}$  of  $\epsilon''(\nu)$  peaks at (a)  $441 \text{ cm}^{-1}$  and (b)  $570 \text{ cm}^{-1}$ , and that of the relative damage threshold in dependence of the abrasion particle size. The numbers indicate the stages of treatment: (1)  $40/28 \mu\text{m}$ , (2)  $5/3 \mu\text{m}$ , (3)  $3/2 \mu\text{m}$ , (4)  $1/0 \mu\text{m}$ , (5)  $0.5/0 \mu\text{m}$ , (6)  $0.3/0 \mu\text{m}$ , (7)  $0.1/0 \mu\text{m}$ ; (8) refers to the natural face. (c) Histogram of optical strength relative to abrasive particle size.

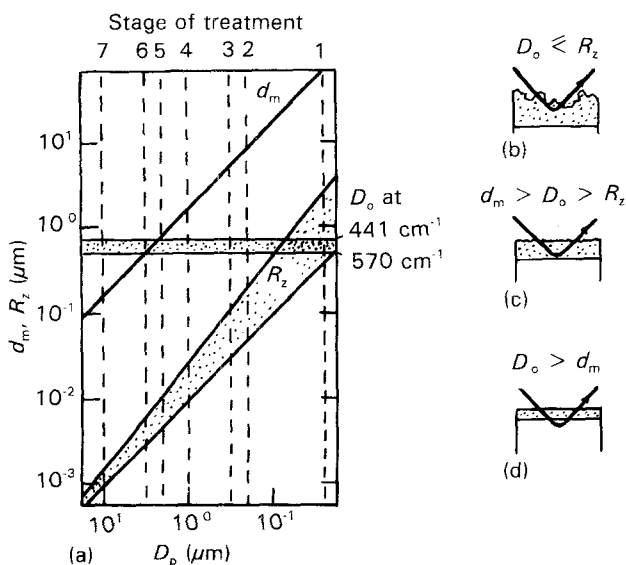


Figure 5 Thickness and relief height of the surface layer modified by grinding of a sample depending on the abrasive particle size.

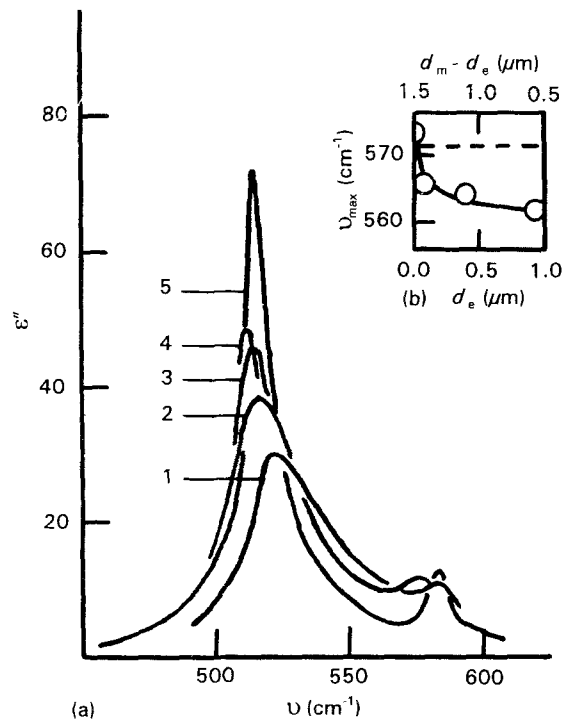


Figure 6 (a) Spectra  $\epsilon''(\nu)$  of sapphire polished with  $1/0 \mu\text{m}$  powder (1) and then etched by  $\text{Ar}^+$  ions with removing the layer of thickness  $d_e = 0.1 \mu\text{m}$  (2),  $0.4 \mu\text{m}$  (3),  $0.9 \mu\text{m}$  (4). If the remaining layer is less than  $D_o$ , the bulk contributes to the spectrum (5). (b) Variation of  $\nu_{\max}$  versus the thickness of removed (or remaining) layer; (---) the position of  $\nu_{\max}$  in the spectrum of the natural face.

in the spectrum of a polished sample ion-etched step-by step. The decrease of  $\nu_{\max}$  when opening the deeper sub-surface layer, gives evidence of the existence in it of strain deformation, whereas on the surface, the compressional deformation dominates. (The latter fact is derived from the comparison of  $\nu_{\max}$  with the band position in the spectrum of undistorted natural face, Fig. 6b.) When the removed layer becomes more than  $\sim 1 \mu\text{m}$ , the infrared light penetration depth exceeds  $d_m$ , and again the bulk contributes to the reflection beam. This is revealed in the spectrum by the drastic increase of the intensity of the band and by the high-frequency shift of  $\nu_{\max}$ .

The respective histogram in Fig. 4c shows the monotonic growth of the optical strength. With decreasing powder grain size,  $Q_{\text{th}}$  first increases and then remains nearly the same. Thus the optical strength of the sapphire surface is determined by a thin (not more than  $0.15 \mu\text{m}$ ) layer remaining after the last stage of polishing. The optical strength of the natural face as well as of the ion-etched surface, which are free of modified layers, is substantially higher than that of the polished surface (Table I).

Other experimental data also demonstrate the effect of structural imperfection on the optical strength of the sapphire. Table II gives the  $Q_{\text{th}}$  values obtained for two samples which have a similarly treated surface (deep polishing with a final powder grain size of  $1/0 \mu\text{m}$ ), but prepared from single-crystal preforms of different quality. Significant structural imperfection in one of the samples was indicated by the appearance of the infrared band at  $590 \text{ cm}^{-1}$  (Fig. 7). This band occurs in the spectrum of  $\alpha\text{-Al}_2\text{O}_3$  due to substantial

TABLE II Damage threshold of the  $\alpha\text{-Al}_2\text{O}_3$  samples cut from different crystal preforms. The infrared spectra of Samples A and B are shown in Fig. 7

Sample	Power density, $Q_{th}$ (rel. units)	
	Bulk	Polished surface
A	1.0	0.5
B	0.4	0.3

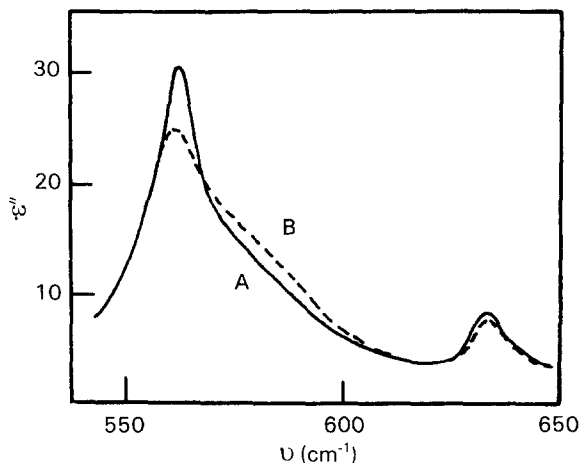


Figure 7 Spectra  $\epsilon''(\nu)$  of two samples, A and B, both polished with  $1/0\ \mu\text{m}$  powder but cut from different preforms. Their optical strengths are given in Table II.

internal deformation of the crystalline lattice [1]. It can be seen in Table II, that the sample cut from a more perfect preform has higher optical strength, both in the bulk and on the surface.

The correlation between optical strength and spectroscopic parameters also appears for the natural faces of various crystals having significant dispersion of their structural properties.

### 3.1.3. Laser modification of the surface

During investigation of the effect of lattice distortion on the optical strength by determining the single-pulse threshold, the structure of a crystal as well as its surface profile are defined by the sample history; changes occurring in the material under the action of laser radiation being out of the scope of this experiment. At the same time, the routine operating of the power optics is connected with the multiple sub-threshold irradiation of a target under the condition  $Q < Q_{th}$ . In this case, the laser-induced changes in the properties of a crystal are as important as the preliminary treatment. Therefore, it is useful to study the behaviour of structural properties in sapphire subjected to laser radiation by a single or by a series of sub-threshold pulses.

We studied the sub- and super-threshold interaction of light with the natural and polished surface, and with the annealed polished surface. The natural face was irradiated by eight pulses produced by laser 2 at power densities of  $0.25Q_{th}$ ,  $0.75Q_{th}$  and  $Q_{th}$ . Changes in the infrared spectrum are seen in Fig. 8.

In all cases the sub-threshold irradiation leads to a growth in intensity and to a decrease in the half-width of the  $570\ \text{cm}^{-1}$  band, while the super-threshold irradiation results in a decrease of the intensity and an increase in the half-width of the band; the "defect" band in the range near  $590\ \text{cm}^{-1}$ . The features of the spectrum obtained after irradiation of the surface at  $Q = Q_{th}$  allow one to conclude that the structure of the natural face becomes close to the structure of the polished surface, i.e. quasi-amorphization takes place. Irradiation at  $Q < Q_{th}$  is revealed in the opposite way: the crystalline structure becomes more ordered.

The action of the laser radiation on the polished surface at  $Q \geq Q_{th}$  was not indicated in the spectrum. At  $Q < Q_{th}$  the changes are insignificant (Curves 6, 7, Fig. 8), although an increase in the intensity of the  $570\ \text{cm}^{-1}$  band evinces some structural ordering. A shift of the band maximum is due to local deformations of the crystalline lattice.

Finally, irradiation of the annealed surface at  $Q \geq Q_{th}$  is equivalent (from the viewpoint of infrared spectroscopy) to irradiation of the natural face; at  $Q < Q_{th}$  it is not sensed by this method.

In general, one can conclude that the sub-threshold irradiation causes the surface to be perfected. This

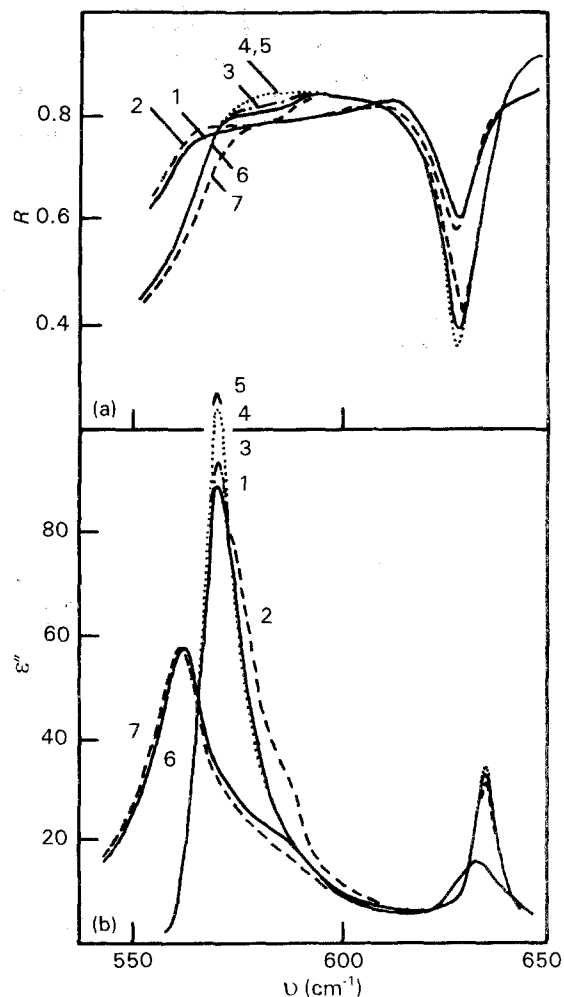


Figure 8 Changes in (a) the reflectivities and in (b)  $\epsilon''(\nu)$  spectra of the natural face (1-5) and of the polished surface (6, 7) subjected to irradiation under the following conditions: (1, 6) before irradiation; (2)  $Q = Q_{th}$ ,  $N = 1$ , laser 2; (3, 7)  $Q = 0.75Q_{th}$ ,  $N = 8$ , laser 3; (4)  $Q = 0.75Q_{th}$ ,  $N = 8$ , laser 2; (5)  $Q = 0.25Q_{th}$ ,  $N = 8$ , laser 3.

result, obtained by reflection spectroscopy and relating to the surface layer of  $\sim 1 \mu\text{m}$  thick, was earlier found by means of the low-energy electron diffraction (LEED) method applicable to the 1–2 surface monolayers of the natural face of the  $\alpha\text{-Al}_2\text{O}_3$  crystals [11].

### 3.2. Laser damage

#### 3.2.1. Multiple-pulse LID

Structural ordering observed in sapphire subjected to the sub-threshold irradiation, is quite unexpected. It is widely accepted that multipulse irradiation of transparent dielectrics causes a nucleation of latent damage sites in them [11–13], the accumulation of which finally induces breakdown and macroscopic failure. Glebovski *et al.* [14] reported the cumulative process in dispersed  $\gamma\text{-Al}_2\text{O}_3$  which is the crystalline material with the physical properties close to  $\alpha\text{-Al}_2\text{O}_3$ , and chemically identical to it. The mass-spectroscopy method indicates the yield of fragments of  $\text{AlO}$ ,  $\text{Al}_2\text{O}$  and  $\text{AlO}_2$ , in the results of the sub-threshold irradiation. However, the sub-threshold decomposition observed by Glebovski *et al.* [14] does not correlate with the infrared spectroscopic and LEED [11] data on the ordering of the sapphire structure.

The question of which of these two factors (destruction or ordering) is dominant in the material irradiated with sub-threshold dose, is answered directly from the multiple-pulse LID experiment.

Pulse train was interrupted when macro-damage of the sample occurred, or when the number of pulses reached  $10^4$ . Irradiation of both the surface and the bulk, yields the effect of the sub-threshold damage. Fig. 9 represents some  $N$  versus  $E$  curves plotted on a semi-logarithmic scale (where  $N$  is the number of pulses needed to obtain a macroscopic defect and  $E$  is the electric field strength in a pulse). There are no grounds to consider that the accumulation effect is due to the inclusions alone. In testing the samples fabricated by the Verneuil technique (which provides fewer impurities), one obtains a dependence of  $N$  on  $E$  differing from that revealed by the KMM-prepared samples, in that they have greater strength at the same  $N$  and less scatter of the values. The behaviour of the curves,  $\log N$  versus  $E$ , for the surface and for the bulk of all samples is the same: the total life-time up to the damage,  $\tau = t_p N$ , grows exponentially as the field strength drops.

#### 3.2.2. Mechanism of LID

The present work was not aimed at investigating the mechanism of the laser-induced destruction in  $\alpha\text{-Al}_2\text{O}_3$ , because this problem may be solved just by detailed experimental studies of the optical resistance depending on temperature, time, frequency, etc. Thus we restrict ourselves to particular remarks.

The time dependence of optical resistance in sapphire indicates the kinetic character of the irreversible degradation of the material under the action of the sub-threshold pulses: a fact which is in agreement with the results of the mass-spectroscopic investigation [14], but which is in contradiction with the results

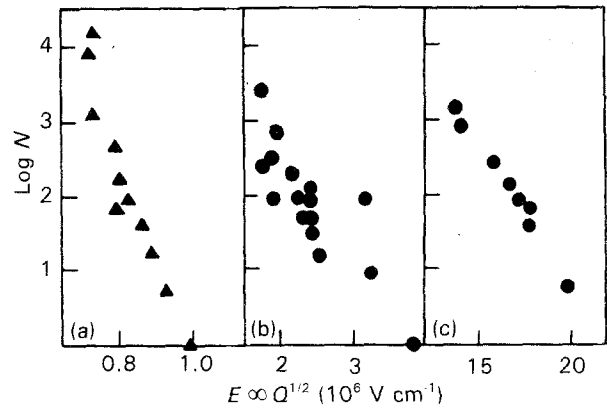


Figure 9 The number of pulses required to produce damage versus electric field strength in a pulse for (a) a natural face and (b) bulk  $\alpha\text{-Al}_2\text{O}_3$  single-crystals grown by (a, b) KMM and (c) Verneuil techniques. Here  $d_{cr}$  is (a)  $120 \mu\text{m}$ , (b)  $15 \mu\text{m}$  and (c)  $13 \mu\text{m}$ . (b, c) Laser 1 and (a) laser 3 were used.

obtained by the infrared spectroscopy and LEED methods [11]. This contradiction may be eliminated if one assumes that both processes (degradation and structural ordering) occur simultaneously, but that different experimental methods are sensitive to only one of these processes. Thus, mass-spectroscopy displays the evolution of localized origins of destruction. The infrared spectroscopy and the LEED method are less sensitive to local defects and indicate the integral effect of structural ordering, which is not registered by the mass-spectroscopy method.

In the case of sub-threshold radiation, the local defect centres (for which the pulse power density exceeds the “dangerous” level) arise and develop simultaneously with the total perfection of a crystal structure (decreasing density of dislocations, relaxation of local stresses of deformation, etc.)

The experimentally observed exponential dependence of  $\tau$  on  $E$ , is indicative of the thermal fluctuation mechanism of destruction [15] which suggests the ensemble of local defects arising and evolving under the action of laser radiation. Nucleation of elementary defects, with the help of thermal density fluctuation, implies the existence in a solid of inhomogeneities having an intrinsic vibrational spectrum. Foreign inclusions of sub-micrometre size may form part of these inhomogeneities. However, as theoretically estimated [16], for the nucleation of the initial defect in  $\alpha\text{-Al}_2\text{O}_3$ , it is sufficient for spontaneous thermal fluctuation of density to be comparable in dimensions with the thermal phonon path (which is  $\sim 5 \text{ nm}$  in  $\alpha\text{-Al}_2\text{O}_3$  [17]) occurring in the focal spot of the laser beam. These large-scale fluctuations are the intrinsic dynamic inhomogeneities. Thus the thermal fluctuation mechanism of laser-induced destruction is quite real in sapphire. The absorbing micrometre-scaled inclusions do not take part in the accumulation process, because if they occur in the focal spot, the macro-damage develops through thermal explosion or through an electron avalanche stimulated by the absorbing particles [18]. During the multiple-pulse irradiation, impurities effect a decrease of the average number of shoots needed for breakdown and an in-

crease of the scattering of the measured values. In our experiment this is seen from a comparison of the data obtained for the samples prepared by the Verneuil technique and for the KMM (Fig. 9).

#### 4. Conclusion

The action of laser radiation on a transparent dielectric may lead to both degradation and perfection of a crystal lattice. The former effect is usually associated with the laser-induced damage of a solid, and the latter is related to the laser annealing. It is rather difficult to distinguish both these processes, a fact which complicates practical problems of laser treatment of materials.

In sapphire, the above-mentioned processes occur simultaneously: the general structural ordering is accompanied by the development of local origins of destruction, in which a breakdown and macro-damage are induced by a number of sub-threshold laser pulses. A nucleation of elementary defects might be assigned to absorbing impurities existing in manmade crystals of  $\alpha\text{-Al}_2\text{O}_3$ . However, it is found that the optical strength is even sensitive to the extent of ordering of a crystal. The samples with an initially more perfect crystal lattice, reveal higher optical strength. This correlation is true not only for the bulk, but also for the surface layer, disturbed by mechanical polishing: the treated surface layer retains a "memory" of the initial structure. If the optical strength was determined by the impurities statistics only, the dependence on structure would not be revealed by the experiment.

The infrared spectroscopic data indicate that the submicrometre surface layer of the polished sapphire crystal is a non-equilibrium (not relaxed) amorphous-like substance. In our opinion, low optical strength of

the polished surface in comparison with that of the naturally grown face, is mainly caused by a disorder in the structure rather than by inclusions embedded during polishing.

#### References

1. A. S. BARKER, *Phys. Rev.* **132** (1963) 1474.
2. M. I. MUSATOV, *Optiko-mekh. prom. (Sov. J. Glass Technol.)* **8** (1975) 36.
3. W. E. LEE, K. P. D. LAGEROF, T. E. MITCHELL and A. H. HEUER, *Philos. Mag. A* **51** (1985) L23.
4. C. R. GIULIANO, *Appl. Phys. Lett.* **21** (1972) 39.
5. A. S. BEBCHUCK, D. A. GROMOV and V. S. NECHITAILO, *Kvantov. Elektron. (Sov. J. Quant. Electron.)* **3** (1976) 1814.
6. D. MILAM, *Appl. Optics* **16** (1977) 1204.
7. A. A. KRAVCHENKO, Yu. I. LOKHOV and D. I. CHEREDNICHENKO, *Fiz. Khim. Stekla (Sov. J. Glass Phys. Chem.)* **16** (1990) 923.
8. V. M. ALTSHULER, E. N. BABADJYAN and V. V. KOSACHEV, *Fiz. Khim. Obrabotki Mater.* **6** (1983) 174.
9. M. E. DOVGAN, V. I. ZAITSEVA, M. I. SHACHNOVICH, *ibid.* **4** (1976) 146.
10. I. P. BABIJCHUK, E. R. DOBROVINSKAYA, L. A. LITVINOV and A. P. RADCHENKO, *Optiko-Mekh. Prom. (Sov. J. Glass Technol.)* **3** (1988) 57.
11. A. CHMEL, S. B. ERONKO, S. A. KNYAZEV, N. M. LEKSOVSKAYA and M. I. MUSATOV, *Poverkhnost* **1** (1992) 137.
12. D. KITRIOTIS and L. D. MERKLE, *Appl. Optics* **28** (1989) 949.
13. S.-T. WU and M. BASS, *Appl. Phys. Lett.* **39** (1981) 948.
14. A. A. GLEBOVSKI, I. F. MOISEENKO and A. A. LISICHENKO, *Izv. Akad. Nauk SSSR (Bull. Acad. Sci. USSR, Phys. Ser.)* **53** (1989) 568.
15. S. N. ZHURKOV, V. A. PETROV, A. M. KONDYREV and A. E. CHMEL, *Philos. Mag. B* **57** (1988) 307.
16. A. KUSOV, A. KONDYREV and A. CHMEL, *J. Phys. Condens. Matter* **2** (1990) 4067.
17. C. L. TANG, *J. Appl. Phys.* **37** (1966) 2945.
18. N. BLOEMBERGEN, *Appl. Optics* **12** (1973) 661.

Received 27 April 1992

and accepted 3 February 1993